PAPER • OPEN ACCESS

Nuclear data for fusion: inventory validation successes and future needs

To cite this article: Mark R Gilbert 2023 *J. Phys. Energy* **5** 034002

Journal of Physics: Energy

Nuclear data for fusion: inventory validation successes and future needs

Mark R Gilbert [ID]

United Kingdom Atomic Energy Authority, Culham Centre for Fusion Energy, Culham Science Centre, Abingdon, Oxon OX14 3DB, United Kingdom
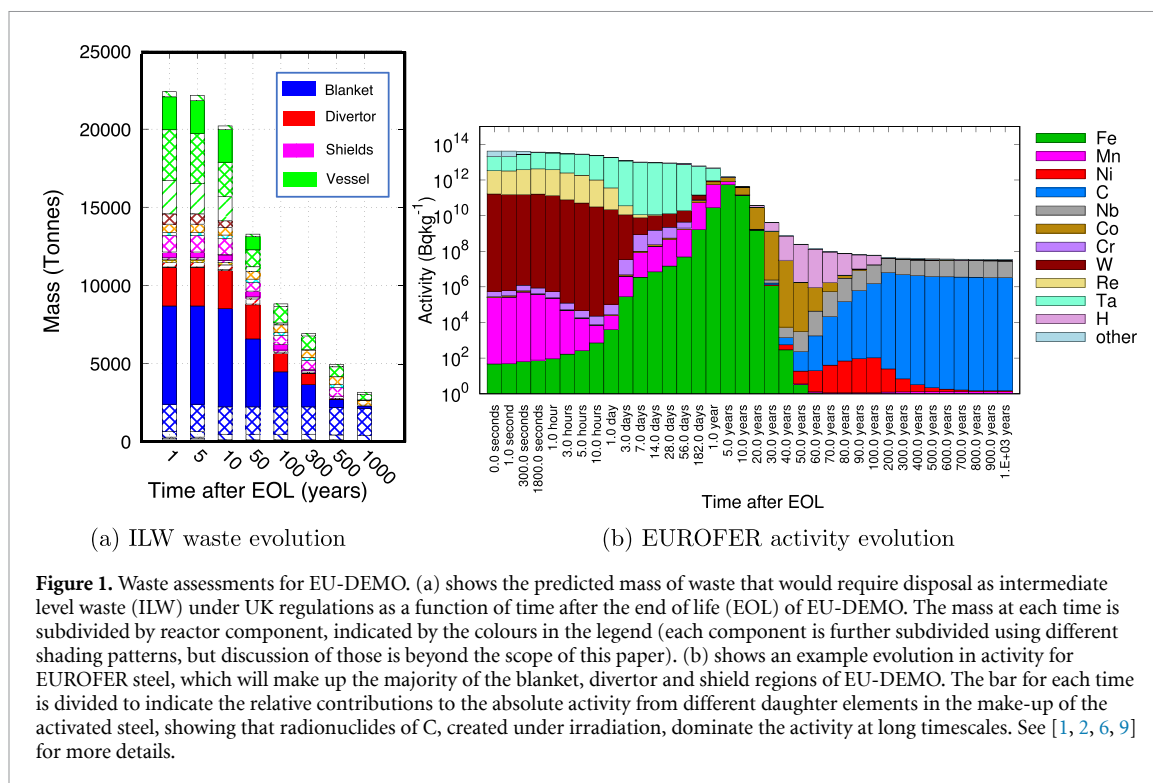
E-mail: mark.gilbert@ukaea.uk

Abstract

Nuclear data, describing neutron reaction probabilities (cross sections) and decay behaviour, are critical to the design and operation of fusion experiments and future fusion power plants. Equally vital, are the inventory codes that use the data to predict neutron-induced activation and transmutation of materials, which will define the radiological hazards that must be managed during reactor operation and decommissioning. Transmutation, including gas production, combined with the neutron-induced displacement damage, will also cause the properties of materials to degrade, for example through swelling and embrittlement, eventually limiting the lifetime of components. Thus validated and accurate nuclear data and inventory codes are essential. For data validation there are decay heat measurements performed at FNS in Japan more than 20 years ago. The experiments produced an invaluable database for benchmarking of nuclear data libraries; the latest versions of several international libraries perform well against this data during tests with the FISPACT-II inventory code, although there is still scope for improvement. A recent attempt to provide fusion-relevant validation based on γ-spectroscopy data from neutron-irradiated material samples tests produced predictions for short-lived (several hours or less) radionuclides. The detailed analysis performed for molybdenum demonstrates how these data could eventually provide a new benchmark, and also illustrates the potential benefits of further experiments targeting the longer-lived radionuclides relevant to maintenance and decommissioning timescales. There are also some successful tests of transmutation predictions with FISPACT-II. These direct validations of inventory simulations are critical for lifetime predictions and future experiments should learn lessons from the examples described for tungsten, which demonstrate the importance of an accurate description of the neutron spectrum in experiments. More novel experimental techniques are needed to measure helium production in materials such as Fe and C, but the need to validate the nuclear data evaluations used by simulations should motivate future experimental efforts.

1. Introduction

Designing the next generation of fusion experimental facilities and prototype power plants requires detailed predictions of the nuclear response of materials. In particular, engineers need to design the plant operation, maintenance and decommissioning with accurate knowledge of the neutron-induced activation of the materials being proposed for regions within the vacuum vessel of magnetic confinement fusion tokamaks (and inside the vessel/chamber of any other fusion concept where neutrons are produced), where the neutron exposure will be highest. For example, computational assessments are vital to understand the radioactive waste arisings that can be expected at the end-of-life (EOL) of future fusion reactors, with results of the severity [1, 2] and volumes [3, 4] of waste being used to drive design refinement [5], consideration of alternative materials [6], and even review of the approach to classification of fusion waste [7]. For example, figure 1(a) illustrates outputs from whole reactor waste assessment predictions for the European

(a) ILW waste evolution   (b) EUROFER activity evolution

Figure 1. Waste assessments for EU-DEMO. (a) shows the predicted mass of waste that would require disposal as intermediate level waste (ILW) under UK regulations as a function of time after the end of life (EOL) of EU-DEMO. The mass at each time is subdivided by reactor component, indicated by the colours in the legend (each component is further subdivided using different shading patterns, but discussion of those is beyond the scope of this paper). (b) shows an example evolution in activity for EUROFER steel, which will make up the majority of the blanket, divertor and shield regions of EU-DEMO. The bar for each time is divided to indicate the relative contributions to the absolute activity from different daughter elements in the make-up of the activated steel, showing that radionuclides of C, created under irradiation, dominate the activity at long timescales. See [1, 2, 6, 9] for more details.

demonstration fusion power plant (EU-DEMO), which are only possible with comprehensive nuclear data libraries used by modern and efficient nuclear inventory codes [8].

In some cases, the material and component lifetimes can be impacted by the neutron-induced transmutation (change in chemical composition), even before the radio-activation is taken into account; early removal of components to reduce severe activation and avoid difficulties in handling and decommissioning is a possible solution to the waste challenges faced by fusion, and hence could also be considered as life-limiting. Mechanical, structural and other functional properties of the materials are influenced, sometime detrimentally, by changes in composition. For example, rhenium (Re) concentrations of a few atomic % in tungsten (W), which is a reasonable expectation from predictions of the EOL chemical make-up of W armour tiles in the first wall of the EU-DEMO first-of-a-kind (FOAK) fusion power plant [10], have been shown to significantly reduce the thermal diffusivity, and hence thermal conductivity, of W [11], which could significantly alter the ability of armour tiles made of W from performing the necessary heat removal to avoid melting. There is even emerging evidence that the clustering of transmutation products might impact the performance of the reduced-activation ferritic-martensitic (RAFM) steels being designed for fusion applications [12], despite the fact that transmutation rates are relatively low in these materials (certainly compared to W). On the other hand, it is well-established that the production of gas, hydrogen and helium, via transmutation reactions, can lead to embrittlement and swelling in steels [12, 13], while helium is known to reduce the strength of welds if present in the steel being welded at concentrations as low as ten parts per million [14, 15], and so accurate prediction by nuclear codes of the gas production rates under neutron irradiation is needed to determine the lifetimes of materials.

Reliable nuclear data and high-fidelity in the codes that use them to make transmutation, activation, and transport predictions is critical. Nuclear data, often taking the form of application-specific libraries, are used throughout the fusion reactor lifecycle: from the design phase where transport simulations and inventory (burn-up) calculations are used to predict the shielding efficacy, tritium breeding performance, and radiological hazard of a design; through construction, where those same calculations must be refined and qualified using the as-built configurations to satisfy regulators and gain permissions to operate; to operations, where many of the diagnostics rely on good nuclear data to measure plasma performance; and finally to maintenance and decommissioning, where activation predictions must be accurate to enable the planning of remote handling activities and waste management.

This paper reviews UKAEA efforts to validate nuclear data libraries and test nuclear inventory codes, which predict transmutation, using available experimental data. Recent efforts to perform nuclear data experiments using γ-spectroscopy for fusion relevant elements including Mo are also presented, highlighting the challenges faced when trying to repurpose ageing facilities to obtain high quality irradiations and

measurements. We also discuss some rare, successful benchmarking of transmutation predictions from inventory simulations; for W in fission test reactors. Below we begin by discussing an extensive and important fusion-relevant test suite based on experimental decay-heat measurements.

The needs of future nuclear data measurements and benchmark experiments for fusion inventory simulations are discussed throughout the paper because these will help to reduce uncertainty in code predictions and to minimise engineering safety factors (which are costly), which is highlighted by some deficiencies in cross sections that lead to helium production in Fe and C.

2. Nuclear data and inventory benchmarks

2.1. FNS decay-heat measurements

At the end of the last century, from 1996–2000, a series of experiments were performed at the Japan Atomic Energy Agency's fusion neutron source (FNS) [16, 17]. For almost two decades, this benchmark has been used to test the quality of nuclear data for fusion applications (see, for example, [18–22]); it has been applied to qualify nuclear data libraries for use in activation calculations on both ITER and EU-DEMO.

Full details of the experimental methodology and process by which the data is used as a simulation benchmark are given in [21, 22]. A total of 73 different materials were irradiated for either 5 min or 7 h in the 14 MeV FNS source and the total heat output from each sample was subsequently measured over periods of minutes or days, for the shorter and longer irradiation experiments, respectively. There is good provenance and data quality, allowing faithful reproduction of the experiments via simulation, which is done at UKAEA using an automated script, allowing the benchmark simulations, plots, and statistical comparisons to be performed within minutes (more detailed analysis of each material, as presented in the technical reports [22] can take longer due to the inherent subtlety in each experiment, see the examples discussed in [21]).

Figure 2 shows two typical comparisons from the benchmark. The top graphs show the total decay-heat data measurements (as data points) alongside the curves obtained from FISPACT-II simulations with several different general-purpose nuclear cross section libraries for stainless steel grade 316 (a) and elemental osmium (b). FISPACT-II [8] is an inventory code for predicting composition evolution of materials under irradiation, which has been developed at UKAEA for almost three decades. For SS316 in figure 2(a), the performance of the simulations in capturing the total decay-heat evolution following a 7 h irradiation is excellent for all nuclear libraries. This is an impressive validation of the inventory calculations because of the number of contributing nuclides that must be correctly predicted to produce the right total at each measurement. The lower panel associated with this experiment, figure 2(c), which shows the underlying contributions to the TENDL-2021 [23] total from evolving (decaying) individual radionuclides, demonstrates that the contributions from seven different nuclides, with different fractional contributions as a function of time, must be properly represented in both magnitude (determined by the reaction cross sections) and profile (determined by decay data) to produce the good match.

However, figures 2(b) and (d), for Os, which requires accurate inventory predictions due to its importance as a transmutation element in W [21], demonstrate that the comparison is not always so good. The decay-heat experimental data in this case are poorly captured by the simulations and, even worse, there is significant disagreement in the profiles and magnitudes of predictions by different libraries, which makes it difficult to assess the cause of the disagreement to experiment and thus to consider remedies. The nuclide breakdown for the TENDL-2021 simulations in figure 2(d) do at least give some clues; as discussed previously in conjunction with EAF2010 [21], the profile of the ^{190m}Os radionuclide, with a half-life $T_{1/2}$ of 9.9 min, appears to have the right evolution profile for the total decay-heat measured. A previous benchmark report [24], noted the EAF2010 partial success, and this directly led to improvements in the next release of TENDL, TENDL-2019 [25], which also benefits TENDL-2021 here. Further adjustments (reduction) of the cross section for the production of ^{190m}Os via inelastic scattering alongside changes to the production of the minor radionuclides could solve the remaining over-prediction in figure 2(d).

Figure 3 demonstrates the overall benchmark performance of several nuclear data libraries against the decay-heat data. Average C/E values—arithmetic mean of the ratios of the Calculated decay-heat values to the Experimental measurements at each acquisition time—are shown in figure 3(a). These indicate that the predictions with the latest TENDL (TALYS-Evaluated Nuclear Data Library developed at IAEA and PSI, Switzerland) and JEFF (Joint Evaluated Fission and Fusion File produced via an international collaboration of NEA Data Bank participating countries) libraries, TENDL-2021 [23] and JEFF-3.3 [26, 27], respectively, as well as the 2010, and last, version of the older, European Activation File (EAF) [28] developed at UKAEA, are in good agreement with the majority of the experiments. At higher mass numbers, A, the deviations increase, although the experimental uncertainties are also higher (shown by the vertical bars in the figure). Meanwhile, the latest ENDF/B-VIII.0 [29, 30] library from Brookhaven National Lab in the US performs less well than the others, with a significant number of over-predicted calculations in the mass range around 100.
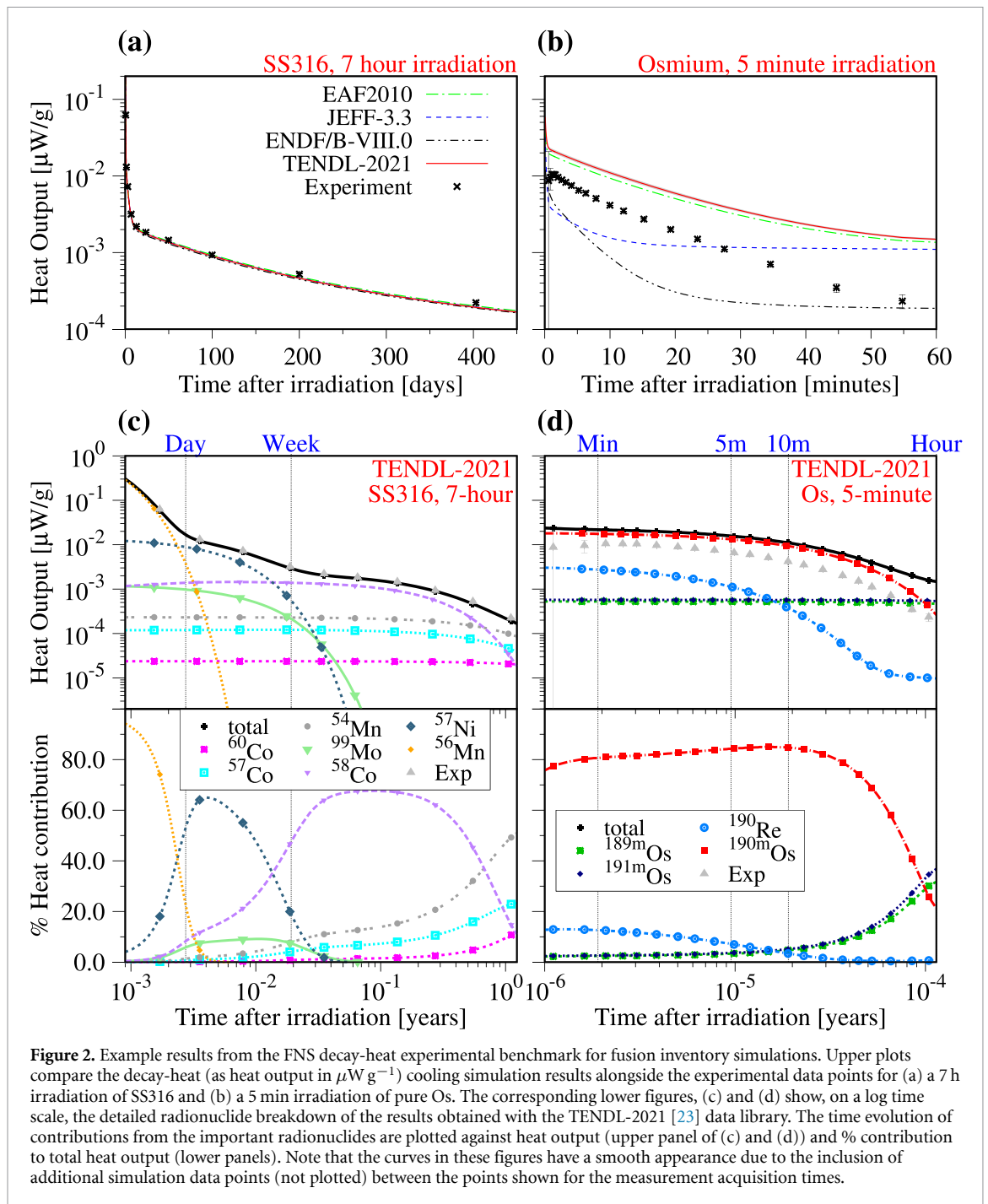
Figure 2. Example results from the FNS decay-heat experimental benchmark for fusion inventory simulations. Upper plots compare the decay-heat (as heat output in $\mu W\,g^{-1}$) cooling simulation results alongside the experimental data points for (a) a 7 h irradiation of SS316 and (b) a 5 min irradiation of pure Os. The corresponding lower figures, (c) and (d) show, on a log time scale, the detailed radionuclide breakdown of the results obtained with the TENDL-2021 [23] data library. The time evolution of contributions from the important radionuclides are plotted against heat output (upper panel of (c) and (d)) and % contribution to total heat output (lower panels). Note that the curves in these figures have a smooth appearance due to the inclusion of additional simulation data points (not plotted) between the points shown for the measurement acquisition times.

This poorer performance is illustrated further by the distribution of reduced-χ^2 statistic values in figure 3(b), where ENDF/B-VIII.0 has a smaller proportion of values below two, while both it and JEFF-3.3 are noted to have more high χ^2 values above 20 than the either EAF2010 or its modern successor, TENDL-2021. For ENDF/B-VIII.0 and JEFF-3.3 some of the large disagreements (clearly visible as outliers in figure 3(a) have been demonstrated [22] to be due to insufficient coverage of target isotopes and reaction channels. It is noteworthy from figure 3(b) that after more than a decade of development the distribution of χ^2 for the latest 2021 version of the automatically generated TENDL library now performs as well as the EAF2010 library that it has largely replaced for fusion applications.

2.1.1. Future decay-heat measurement needs
While the FNS decay-heat benchmark described above is highly valuable, with good provenance and data quality, it is not without deficiencies; it does not contain experiments for some of the key fusion materials, such as RAFM steels that are expected to be used inside fusion reactor vessels and which have a different decay-heat profile than SS316 due to the reduction in long-lived Ni isotopes but increase in production of
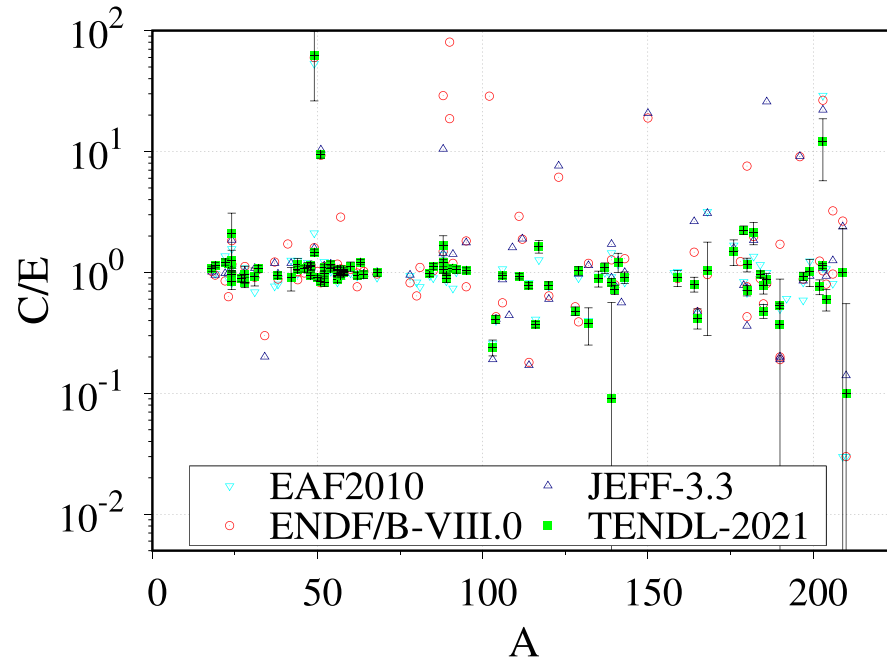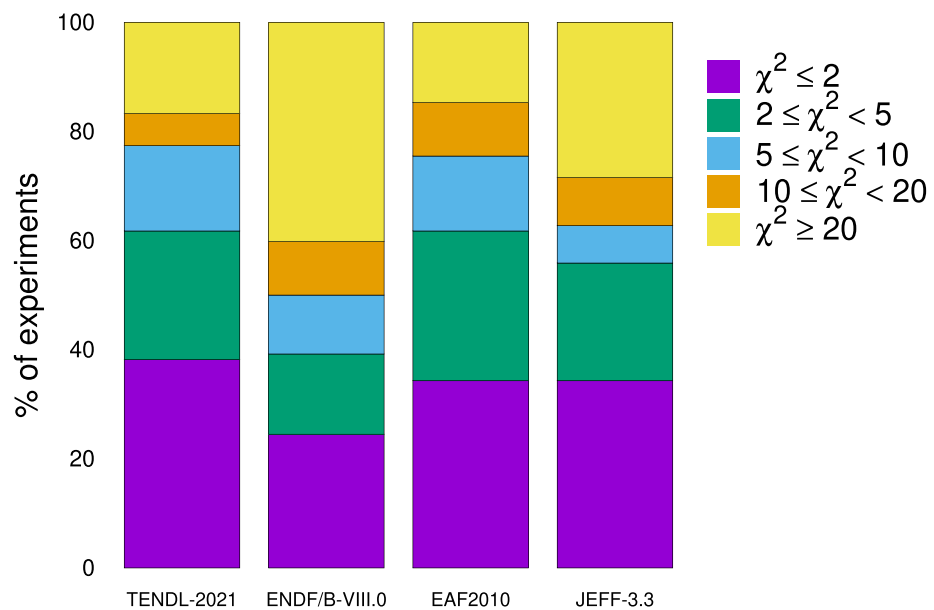
Figure 3. Performance statistics of FISPACT-II simulations with different nuclear data libraries against the FNS decay-heat benchmark database. (a) Shows the average deviation of each library's predictions from the measured data-points of each experiment, plotted against the mass number of the main parent element contained in the experimental sample. For (b), a reduced χ^2 has been calculated for each experiment using the errors reported for each data point. Here the reduced χ^2 is the arithmetic mean of the squares of the differences between the simulated and measured decay-heat points divided by the experimental uncertainty at each measurement. See [22, 27] for further details.

short-lived radionuclides from W [1]. Nor does the existing benchmark include measurements for longer irradiation times. At higher fluxes and longer exposure times, ones relevant to the near-continuous operation regimes of commercial reactors or in the later phases of experimental operation for the future development reactors such as EU-DEMO, a key concern would be the increased production of radionuclides with half-lives of weeks, months, and years, that are only partially explored by the 7 h irradiations in this low-flux benchmark.

Reliable decay-heat predictions remain an ongoing need for fusion; it is critical that simulations are accurate to avoid either under-engineered cooling, which could lead to damage of materials and components, or over-engineering that is both costly and energy-consuming.

2.2. Activity measurements using γ-spectroscopy

In the FNS decay-heat benchmark, the experimental data are global measurements for a material, which means that there is no direct attribution of the decay-heat to a particular radionuclide and its production routes; only by inference, based on the inventory simulations and their input cross section and decay data, can we deduce the dominant radionuclides contributing to the measurements and thus which reactions are validated by the results for a particular experiment. Even then, it is often the case that more than one radionuclide contributes at each measurement time, although one might be overwhelmingly dominant—as demonstrated by the early measurement times for the SS316 experiment (figure 2(b)), where ^{56}Mn contributed around 80% to the total decay heat at the first measurement time (at ∼15 h [22]), with remaining 20% attributed to ^{57}Ni.
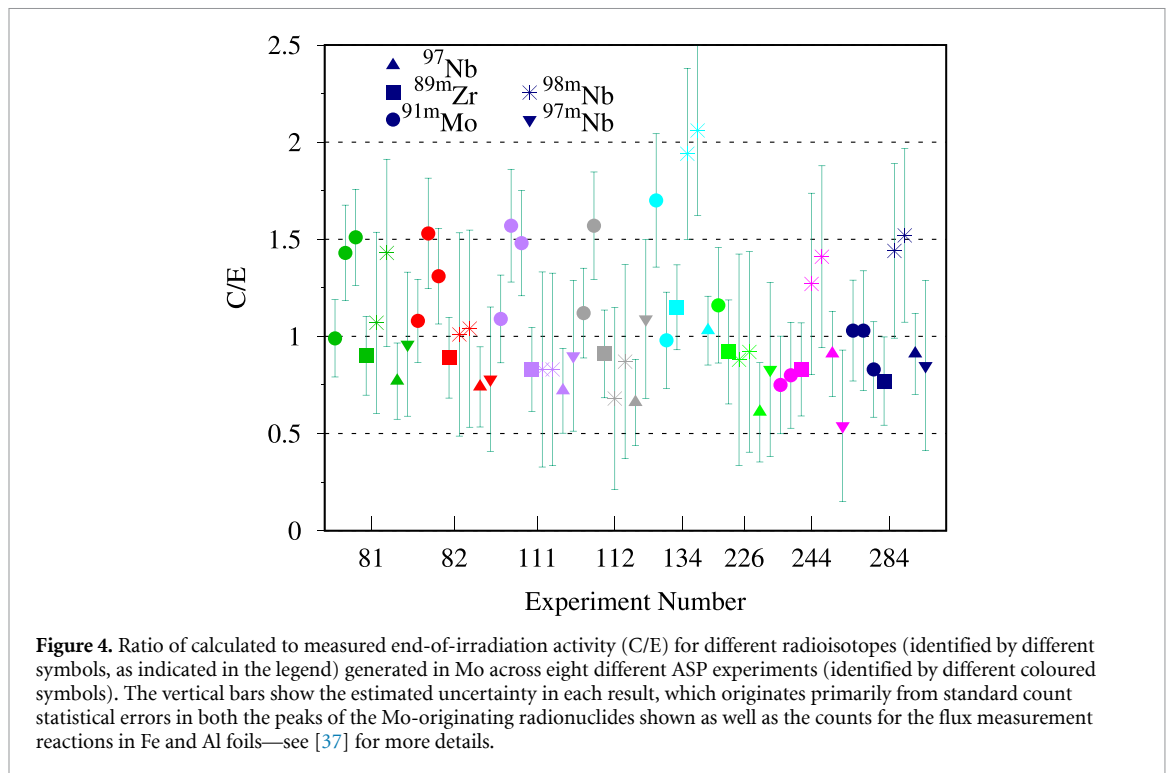
Direct validation of the production of a specific radionuclide, ideally produced by only one, single-step reaction pathway, requires a different experimental approach. For this reason, UKAEA, in the period 2011–2015, undertook a campaign of irradiations at a 14 MeV accelerator source, ASP, hosted by AWE, Aldermaston in the UK [31–34]. More than 300 experiments were performed, involving the irradiation of thin-foil metal samples, which were then rapidly extracted to a high-purity germanium γ-spectrometer. The resulting high energy-resolution γ-spectra contain count-peaks at the characteristic energies for the different radionuclides produced in the material during irradiation as they decay. For radionuclides with well-known γ-emission energies and intensities, it is then possible, by summing the counts in a peak at the characteristic energy (the counts for a γ-emission line broaden into a Gaussian peak in the experiments) to calculate the corresponding activity from that radionuclide at the end of the irradiation, which can then be used to test the predicted activity for that same nuclide from the FISPACT-II code with a given nuclear cross section library.

Several studies have already been performed based on the ASP data, including the development of an analysis tool to automate the extraction and processing of the experimental data [34], which provided early confirmation of the identified radionuclides in the different experiments (i.e. by confirming that the measured decay profile matched the accepted half-life in each case), and preliminary comparison between measured and simulated activity for selected experiments on W, Zn, Ti, Zr, and Sn [32, 35]. An alternative automated approach that uses artificial neural networks to identify peaks in the measured spectra that can be subsequently tested against predictions was recently prototyped [36], but the global assessment of performance it provides based on default assessment parameters has proved challenging to use as the basis of a benchmark that can support nuclear data development. All of these studies served to improve the understanding of the requirements of a more rigorous and tailored analysis for sets of the ASP experiments that can form the basis of a new integral simulation benchmark.

Figure 4 shows the C/E comparison performed in [37] for the radionuclides identified by their peaks in the eight experiments performed for Mo (the eight experiments differ in irradiation times and average fluxes—see [37] for details). Mo is of particular interest for fusion applications as a potential alternative armour material in high heat-flux regions of a reactor [37, 38]. There are relatively large errors shown as vertical bars for each data point, which include contributions from statistical count errors, leading to uncertainties in counts for both radionuclides of interest and the radionuclides uses to estimate flux values using Fe and Al foils. Uncertainties in the TENDL-2019 [25] nuclear data used by FISPACT-II to calculate both the activities (C values) and flux values are also included [37]. Despite the uncertainties, the agreement is generally good, with most calculated values within a factor of two of the experimental measurements (i.e. the C/E values are mostly between 0.5 and 2). There are no strong trends of either underestimation (C/E values less than 1) or overestimation (C/E value greater than 1) for any of the five radionuclides measured, suggesting that the inventory predictions are broadly capturing the response of Mo in these short experimental irradiations.

2.2.1. Future γ-spectroscopy measurements

Further work is underway to analyse the remaining ∼300 experiments (starting with recent analysis of 14 tungsten experiments to test predictions of ^{185}W production [39]) from the UKAEA-ASP campaigns, with the final aim being to turn them into an experimental benchmark that can be used to test the performance of nuclear libraries for a variety of fusion materials—in much the same way that the FNS-decay-heat benchmark described earlier is now used. However, the analysis for Mo [37] confirms the drawbacks of the experiments; they are only able to interrogate the production of short-lived radionuclides due to insufficient counts and consequently low signal-to-noise ratios for radionuclides with longer half-lives. The longest-lived of those identified in figure 4 is ^{97}Nb, with a half-life of only $T_{1/2}$ of 1.23 h, which has limited relevance to fusion reactor operations (except maybe to identify the cooling requirements immediately after shutdown). Meanwhile, the FNS-decay-heat experiments on Mo (see table 2 in [37]) probe the production of longer-lived

Figure 4. Ratio of calculated to measured end-of-irradiation activity (C/E) for different radioisotopes (identified by different symbols, as indicated in the legend) generated in Mo across eight different ASP experiments (identified by different coloured symbols). The vertical bars show the estimated uncertainty in each result, which originates primarily from standard count statistical errors in both the peaks of the Mo-originating radionuclides shown as well as the counts for the flux measurement reactions in Fe and Al foils—see [37] for more details.

nuclides, with ^{91m}Nb the longest with a $T_{1/2}$ of 61 days, which has important applicability to qualify predictions of decay-heat and activity when planning for remote operations during maintenance periods.

To be more relevant to testing nuclear code predictions in scenarios where they will be relied upon during the design of fusion reaction operations, future campaigns at facilities like ASP should include irradiation times of at least hours, with measurement times of days and weeks. Even this would not be sufficient to test predictions of activity at timescales relevant to radioactive waste decommissioning, where, for example for Mo, the typical nuclides of concern—i.e. the ones that determine waste classification at the point of disposal—have half-lives in the 100s or 1000s of year timescales [37]. Extended irradiation times are also challenging at accelerator facilities like ASP or FNS (neither of which are available anymore), which cannot typically be dedicated to one experiment for the necessary extended timescales. Alternatively, larger material samples, combined with longer post-irradiation γ measurements in low background shielded environments and Compton suppression systems (to increase the signal-to-noise ratio), could be used to track the decay of the important longer-lived radionuclides (in Mo these are ^{93}Mo, ^{94}Nb, ^{99}Tc and ^{91}Nb [37]) without the need for longer or higher-flux irradiations.

2.3. Transmutation measurements

The nuclear data benchmarking described so far in this paper has been concerned with the radiological outputs of irradiated materials—either directly, in the form of activity (as in section 2.2) or indirectly via a derived quantity, decay-heat (section 2.1). However, for the inventory simulations tested using these experiments, Becquerel activity and other radiological response metrics, are only derived quantities; the fundamental quantities predicted by the simulations are changes in nuclide concentrations. This process is often called transmutation, although this strictly refers to the change of one element into another, which is again a derived quantity as changes in nuclide distributions are the actual predicted behaviour, and not all changes of nuclide lead to transmutation. In many cases, the dominant transmutant nuclide growth under irradiation corresponds to stable nuclides. For example, in the case of W under fusion conditions, the stable nuclides ^{185}Re and ^{187}Re comprise almost 100% of the composition of transmutant Re produced, with the exact balance between these two stable nuclides varying with the neutron environment [40].

Direct experimental validation of the full transmutation response of a material is challenging because there is no radiological response to measure from stable nuclides. However, there have been two notable successes in the last few years for W, where modern techniques have been employed to accurately identify the concentration of all elements (and nuclides) produced during exposure in fission test reactors. W is the primary material being considered for the plasma-facing armour of magnetic-confinement fusion reactors such as EU-DEMO [5]. However, it is a strongly transmuting element due to high neutron capture cross

Table 1. Transmutation measurements (APT/EDX) and simulations (FISPACT-II) for samples of W irradiated in two different fission test reactors. Re and Os concentrations for each material are given in atomic %. See main text for details. APT measurements for the HFR samples are quoted with uncertainties quantified using a mass-to-charge peak under and over ranging approach [44]. EDX measurements for the HFR samples were performed in [42, 43]. APT analysis of the HFIR samples is described in [46].

Reactor	Sample	Re (at.%)	Os (at.%)
HFR	Single crystal APT	1.26 ± 0.15	0.08 ± 0.02
	Polycrystalline APT	1.09 ± 0.07	0.08 ± 0.02
	Single crystal EDX	1.2	0.1
	FISPACT-II	1.4	0.1
HFIR	Low dose APT	1.63	0.05
	Low dose FISPACT-II	1.66	0.10
	High dose APT	6.38	3.23
	High dose FISPACT-II	8.59	8.99

sections that include giant capture resonances [10, 40]. These changes in composition are expected to be life-limiting for W-based components because they can lead to loss of thermal conductivity (critical in high heat-flux regions) [11] or segregation-induced embrittlement and hardening [41]. Thus, accurate prediction of transmutation in W will be vital for fusion engineering.

Samples of pure W (both single crystal and polycrystalline) were irradiated for 208 full-power days in 2008–9 in the High Flux Reactor (HFR) in Petten, Netherlands, and received a total estimated damage dose of 1.67 displacements per atom (dpa) from a neutron energy spectrum with a typical fission profile peaked at 1–2 MeV and a low-energy peak of thermal neutrons [42–45]. Later, in 2012–13, two single crystal W samples were irradiated to doses of 0.1 ('low dose') and 1.8 ('high dose') dpa, respectively, in the High Flux Isotope Reactor (HFIR) at Oak Ridge National Lab in the US, which has a similar fission neutron energy profile but with typically a more pronounced (dominant) thermal Maxwellian [46]. In both cases, atom probe tomography (APT) was used to measure the composition of the samples after irradiation, while the HFR samples additionally had energy dispersive x-ray (EDX) spectroscopy performed to measure the elemental composition. The measurements were performed after periods of decay-cooling (and at different decay times in the case of the EDX and APT analyses of HFR samples) but the evolution of the samples post irradiation is negligible (based on FISPACT-II simulations).

FISPACT-II inventory calculations were performed to simulate the irradiation (and decay-cooling) in both cases, which were possible due to accurate knowledge of the irradiation histories the samples received over several operational cycles of each reactor, and also through good representation of the neutron environments (see [45, 46] for details). It was particularly critical to obtain the correct neutron spectra for these cases due to the importance of the low energy fluxes (below 1 keV) where the neutron-capture cross sections—the ones that dominate the transmutation in these fission environments—are highest. Early analysis of the HFR samples using a volume-averaged neutron spectrum for the low flux material test location in the reactor produced significant disagreement between the simulations and measurements [40], which was only improved through correct characterisation of the local neutron environment around the samples.

Table 1 shows the simulation versus experiment comparison obtained from these two separate experiments. The table shows the calculated Re and Os concentrations, which are the primary transmutation elements in these fission-spectrum experiments (Ta was also measured in [45], but the observed and simulated concentrations were only around 0.01 atomic %). The comparison of the simulations (performed with TENDL nuclear data libraries) to experiment is generally very good, particularly in the low dose samples irradiated in HFIR. At higher dose in HFIR, there is more deviation from the experiment, potentially because of insufficient characterisation of the experiment-specific neutron environment; only a standard spectrum was use for the calculations, i.e. one which represents the generic or typical environment at the sample location without taking account of any local variation, particularly in the low-energy neutron fluxes, that could of occurred due to the specific set-up of the reactor during the time of the experiment.

Another significant feature of these results is that the FISPACT-II simulations were also used to aid the APT analysis. The standard approach for APT is to use the natural abundances of isotopes of elements when sizing the mass-to-charge-state peaks. However, this is not appropriate in samples that have undergone significant transmutation because the isotope distributions of either the original elements or transmutant ones will not typically follow those natural distributions. The specific isotope ratios predicted by FISPACT-II were used to guide the fitting of the APT data, demonstrating another important benefit of having reliable simulations. In [45], the analysis was even extended to obtain the concentration of individual isotopes by ranging each mass peak individually, and again the comparison to the simulated distribution is remarkable.

2.3.1. Future transmutation benchmarking

The examples described above for W demonstrate that it is possible to perform measurements that can be used to directly validate the inventory evolution of solid transmutants predicted by codes such as FISPACT-II. If these were repeated for the majority of the materials relevant to fusion applications then, assuming the comparison was favourable, there would be a high degree of assurance in the ability to predict life-limiting transmutation effects in materials during fusion power plant operation. Future experiments should target this goal, acknowledging that a key requirement—as it was for the activation benchmarks described earlier—is for the neutron environment in any experiment to be accurately characterised to avoid some of the challenges (only partially mitigated) in the above W examples.

3. Ongoing nuclear data needs: helium production

Accurate prediction of solid transmutants such as Re and Os in W, is not the whole story; many of the neutron-induced reactions that nuclides undergo, particularly at the higher energies associated with nuclear fusion, also lead to the enhanced production of helium and hydrogen gas. The growth in concentration of He, in particular, is known to cause swelling and embrittlement in many materials, including steels such as the RAFM steels being developed for fusion structural applications. While, there is still significant uncertainty in the exact mechanisms by which He might reduce the performance of RAFM steels [12], it is nonetheless clear that as-built fusion reactors will require precise knowledge of the expected He production rates in order to develop planned maintenance schemes and to avoid unplanned failure events that are typically more costly and challenging to rectify. Unfortunately, even for well-studied elements such as Fe, which will largely determine gas production in steels, there can still be surprising deficiencies and variation in the nuclear data relied upon to calculate production rates.

3.1. Helium production in iron

Figure 5 shows the cross section evaluations for He production in ^{56}Fe from the latest releases of the main international nuclear data libraries. ^{56}Fe comprises 91.754% of natural abundance Fe and will therefore be the main isotope in the steels used to construct future fusion reactors. The cross section curves for (n,α) reactions, neutron capture followed by α-particle emission (i.e. ^{4}He, the primary stable isotope of helium), for the JEFF-3.3 [26] and ENDF/B-VIII [29] are a good match to the majority of EXFOR data in the fusion relevant range up to 14 MeV. Note that some recent experimental data from 2019 (the EXFOR points are labelled in the figure with the year of publication) originally appeared to deviate significantly from the general trend of data, but a review of the source data [47] indicated that these data points had been incorrectly inserted into the EXFOR database (and actually correspond to the ^{54}Fe(n,α) cross section). This has now been corrected in EXFOR and the '19' data points in the figure closely match the trend of the other data-sets, but this case highlighted the challenges of maintaining such a large and complex database—EXFOR contains data from more than 24 thousand experiments, encompassing the entire history of nuclear data acquisition.

The 1994 experimental values in the figure come from Sterbenz *et al* [49], where an enriched ^{56}Fe sample was bombarded by a wide range of neutron energies (from 1 to 30 MeV) using a spallation source at Los Alamos National Lab in the US. The experiment did not identify the origin of the ^{4}He particles produced, which were measured using silicon detectors, and so the experiment in fact measured the total (n,Xα) cross sections. This explains why the '94' data points continue to increase beyond 16 MeV, in contrast to the evaluated curves from the data libraries—those higher energy cross sections correspond to the sum of at least two ^{4}He production channels, (n,α) and (n,nα), which is confirmed by the equivalent (n,α) + (n,nα) curve from JEFF-3.3 (ENDF/B-VIII.0 does not contain the (n,nα) channel in the version of the library read by FISPACT-II, potentially indicating a processing issue due to improper adherence to ENDF-6 coding standards [50]). This 1994 [49] experiment is the only one in the EXFOR database with such a complete coverage of the relevant energy range for fusion neutrons, and gives the most confidence to the evaluated libraries.

The curves for TENDL-2021 are less satisfactory, showing a significant under prediction of the cross sections compared to the experimental data, which could have significant engineering implications if FISPACT-II simulations using this evaluation was used to predict steel lifetimes. However, TENDL libraries continue to evolve, and the automated production methodology [51, 52] used to create them enables a more rapid response to adjustment needs, so there is a good expectation that the deviation in figure 5 will be corrected for the TENDL-2023 release.
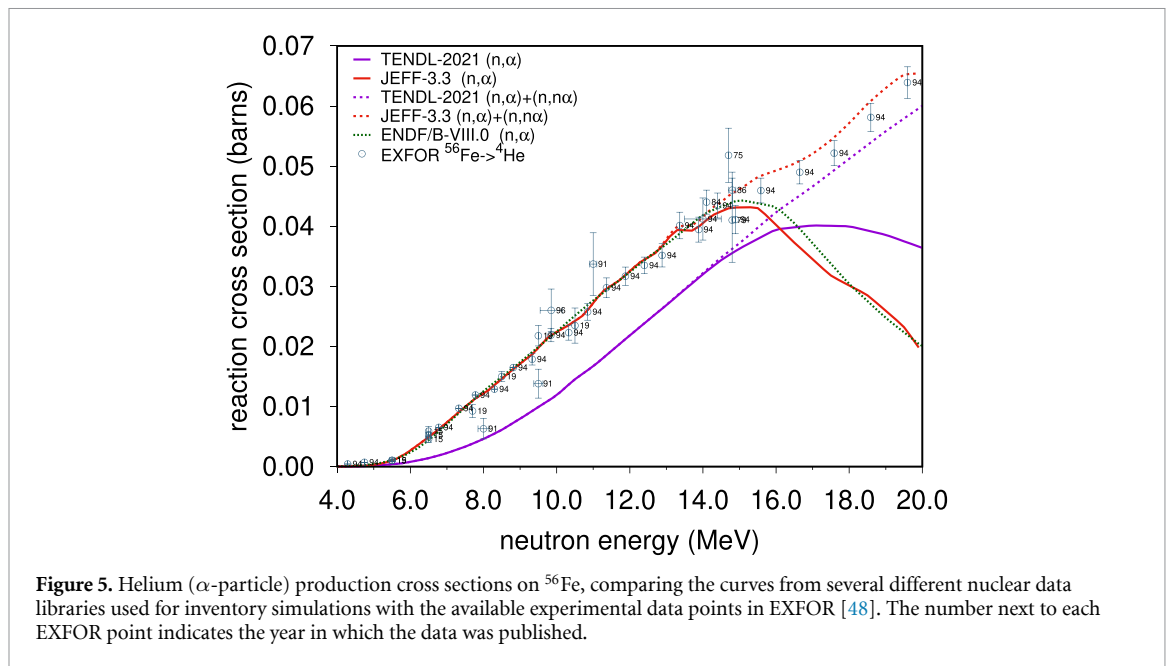
Figure 5. Helium (α-particle) production cross sections on ^{56}Fe, comparing the curves from several different nuclear data libraries used for inventory simulations with the available experimental data points in EXFOR [48]. The number next to each EXFOR point indicates the year in which the data was published.
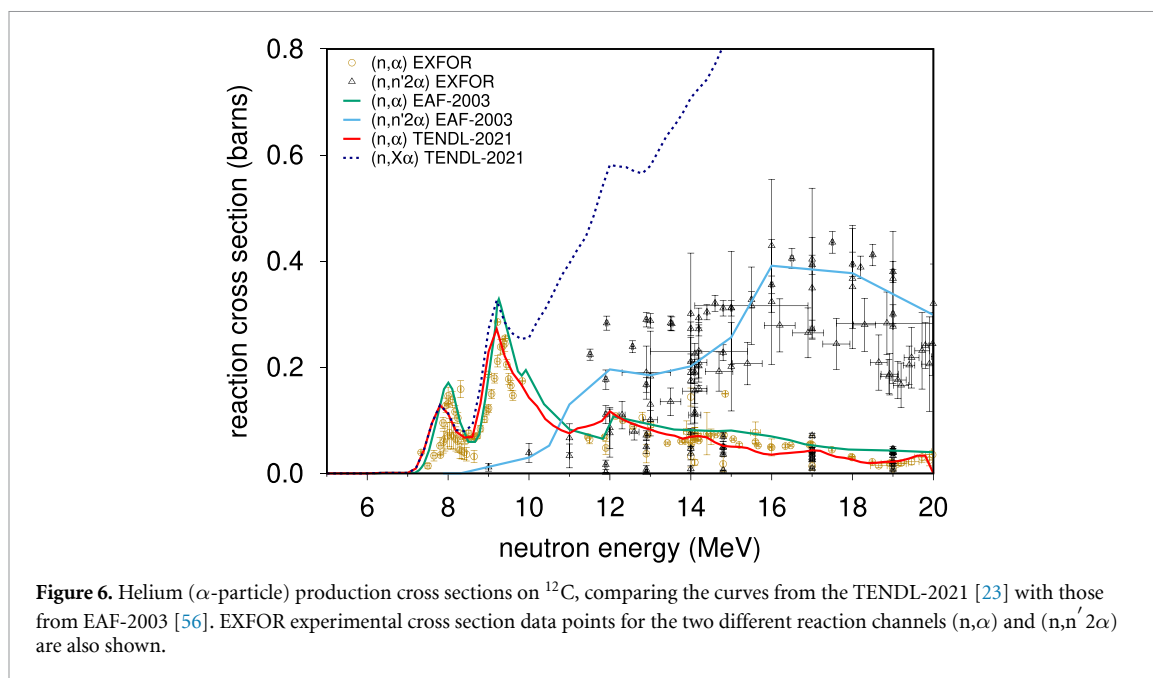
3.2. Helium production in carbon

Carbon has many potential applications in fusion systems. While pure C is no longer favoured as an armour material due to sputtering and tritium retention issues [53], there are potential applications for compounds of carbon, such as W–C as a neutron shield [54] and SiC composites as a high-temperature structural material [55].

However, there is a neutron interaction in carbon that could cast doubt on the suitability of carbon-based compounds for fusion applications. In figure 6, EXFOR cross section data associated with the typical (n,α) channel for He production is shown for the primary stable isotope of C, ^{12}C (98.93% of natural carbon). Also shown, is data attributed to an alternative, more exotic nuclear reaction channel, which involves neutron capture followed by the break-up of ^{12}C into three α-particles and a residual neutron. Typically designated as $(n,n'2\alpha)$ (the third α particle of ^{4}He nucleus is the remaining residual in this convention), the figure shows that there is experimental data that provides strong evidence of a non-negligible cross section for this channel at and around the 14 MeV neutron energies of the deuterium-tritium fusion reaction.

Unfortunately, TENDL-2021 does not include the triple-α production channel, nor do any of the other nuclear data libraries produced in the last decade—at least not in a way that is suitable for inventory simulations. Finding a library that contains this reaction correctly requires the use of the 2003 version of the European Activation File, EAF-2003 [56], which was produced at UKAEA as part of a release of the forerunner to FISPACT-II, EASY [57] and the FISPACT [58] code within it (later EAF versions also contained this unusual channel but the comparison to EXFOR data is very poor).

Figure 6 shows this EAF-2003 cross section curve for $(n,n'2\alpha)$, which is a reasonable fit for the somewhat scattered experimental data. It is interesting to note that the total α production channel $(n,X\alpha)$ in TENDL-2021, also shown in the figure, appears to have features consistent with the EAF-2003 curve for $(n,n'2\alpha)$, albeit at a much higher cross section value. Since $(n,X\alpha)$ is 'total' production it must include the triple production as an effective three-times higher cross section, which is consistent with the comparison of the TENDL-2021-$(n,X\alpha)$ and EAF-2003-$(n,n'2\alpha)$ in the figure. However, a correct $(n,X\alpha)$ is not sufficient to produce accurate inventory evolution as it does not allow for differentiation between reaction channels (e.g. (n,α), $(n,n\alpha)$, and $(n,n'2\alpha)$ could not be reliably separated for ^{12}C from $(n,X\alpha)$).

To see the impact of this apparent omission in modern libraries we can compare ^{4}He production predictions in C under fusion conditions, with and without this additional $(n,n'2\alpha)$ channel. In [59], where a comprehensive response database was created for all elements under EU-DEMO conditions, the predicted He production after 2 years of continuous operation in the first wall of the reactor (corresponding to a flux of 5.04×10^{14} n cm^{-2} s^{-1}) was 410 atomic parts per million (appm) with the TENDL-2015 [60] nuclear data library. Meanwhile, if, instead, the FISPACT-II calculation is repeated with the EAF-2003 cross section data then the predicted He concentration after 2 years is almost an order of magnitude higher at $\sim$3500 appm. Such a predicted difference, if validated, could have dramatic implications for any carbon compound's potential use in a fusion reactor—either the material lifetime will be severely limited due to helium-induced swelling or embrittlement, or the material will require advanced microstructural engineering to allow it to

Figure 6. Helium (α-particle) production cross sections on ^{12}C, comparing the curves from the TENDL-2021 [23] with those from EAF-2003 [56]. EXFOR experimental cross section data points for the two different reaction channels (n,α) and (n,n$'$2α) are also shown.

accommodate high gas production without failure. In any case, the observations here confirm that there must be an effort to reinstate the (n,n$'$2α) for ^{12}C into the next releases of libraries like TENDL, and also that there is a need for further experiments to evaluate this potentially highly impactful reaction channel—the data points are highly scattered in figure 6.

4. Other applications of nuclear data in fusion

This paper has focused on the validation and needs for cross section libraries that predict transmutation of materials via inventory codes. However, this is not the only application for nuclear data within fusion engineering. First, are decay data, whose libraries are an essential component of inventory simulations as they provide the decay rate (or decay constant, proportional to the reciprocal of half-life) of the radionuclides created by neutron irradiation. As well as influencing the transmutation evolution during irradiation, nuclear decay rates control the further evolution of a material inventory after irradiation. Combined with the information provided in decay-data libraries concerning the types (α, β, γ-decay, etc) and energies of decay that radionuclides undergo, these rates determine the radiological outputs of a material, including Becquerels, dose, and (decay) heat, and thus define many of the simulation results discussed in this paper (all of those discussed in sections 2.1 and 2.1 as well as the results shown in figure 1). However, these decay libraries typically receive less validation and verification attention than cross section libraries, with a view within the community that there are no issues to resolve. There has been some recent effort to evaluate the performance and coverage of decay libraries [61], which led to the production of a new recommended file 'decay-2020' [62] for simulations in FISPACT-II. There is a clear need to understand the accuracy of decay-data, particularly as it has a critical role in radiological predictions such as decay-heat and dose-rates.

   Equally critical to understanding the nuclear environment in fusion are the transport simulations that predict how neutrons propagate through the three-dimensional geometry of a reactor. While inventory simulations predict the time evolution of materials due to the neutron fluxes and energy distributions, it is the transport simulations that are typically used to predict those neutron fields as a function of position within a nuclear system. Transport codes, such as MCNP [63] or OpenMC [64], use the same fundamental cross section data as inventory simulations but the important (dominant) reaction channels are instead those associated with elastic and inelastic scattering, neither of which change the parent isotope and thus do not normally contribute to inventory evolution (some inelastic scattering events can convert a nuclide into one of its metastable states leading to a change in radiological output from a material—as discussed for case of Os in section 2.1). The validation of transport simulations and transport nuclear cross section libraries has not been discussed here, although accurate calculation of the neutron flux spectrum is critical to all of the examples discussed. Validation of transport data is nonetheless an area that receives significant attention, including for fusion applications. For example, the validation of simulations used to predict shielding requirements of nuclear reactors has driven projects to create 'shielding benchmarks' for fusion and fission scenarios (see [65] for a recent review), while the need for accurate prediction of tritium breeding with

fusion reactor concepts has motivated tritium breeding ratio benchmarks that test both transport and transmutation modelling (for example, see [66, 67]).

5. Discussion

This paper has highlighted several examples of successful validation of nuclear data libraries and the inventory codes that use them. While the FNS-decay-heat benchmark is an invaluable tool used to test nuclear data libraries it has a limited scope in terms of materials covered, which do not reflect modern fusion needs, and the irradiation and decay timescales considered, which are not representative of fusion power plant operations. The more recent UKAEA-ASP γ-spectroscopy experiments also suffer from issues of insufficient experimental timescales and there is a clear need to expand experimental efforts to target key fusion materials and measure, in particular, radiological responses on timescales relevant to the days, weeks and eventual years of fusion plant operations and years and decades associated with decommissioning activities.

Advancements in composition analysis techniques are providing a promising new route for experimental data on transmutation (burn-up) of materials under neutron irradiation. The potential to perform validation of the complete transmutation predictions from inventory simulations, rather than only testing the part of the calculations leading to a radiological response, will be an important new assurance route for fusion materials. With this new perspective on the potential for direct validation of transmutation predictions, there is scope to revisit historical irradiated materials that have not previously been considered for transmutation measurement, which could now be analysed using advanced techniques such as APT and thus provide a new archive of materials for transmutation validation. However, there is also a need for new experiments to measure transmutation of materials in fusion-relevant environments; the results presented in this paper only demonstrate the successful method with fission-irradiated material, which would also be the case for the majority of historical samples that the technique could be applied to.

Not only are further experiments needed to address the outstanding issues for key fusion materials, but also more careful development of inventory nuclear data libraries to target the specific and unique needs of fusion (e.g. fission reactors are unlikely to be impacted by the He production channels in Fe and C, which are only 'open' at fusion relevant neutron energies). Both integral experiments, for example of decay-heat, and differential cross section measurements are needed. Differential data needs should be guided by the identified priority reaction channels for fusion, such as those identified for W [21] and Mo [37], which should be recorded in an appropriate database of 'needs' such as NEA's High Priority Request List. Whether fusion specific cross section libraries, which previously existed (i.e. EAF) but have now become obsolete, are needed will depend on whether future evolutions of modern general purpose libraries such as TENDL, ENDF/B, and JEFF, will consider more proactively the fusion-relevant energy ranges alongside the ongoing needs of future nuclear fission developments.

Data availability statement

No new data were created or analysed in this study.

Acknowledgments

ORCID iD

Mark R Gilbert ● https://orcid.org/0000-0001-8935-1744

References

[1] Gilbert M R, Eade T, Bachmann C, Fischer U and Taylor N P 2017 Activation, decay heat and waste classification studies of the European DEMO concept *Nucl. Fusion* **57** 046015
[2] Gilbert M R, Eade T, Rey T, Vale R, Bachmann C, Fischer U and Taylor N P 2019 Waste implications from minor impurities in European DEMO materials *Nucl. Fusion* **59** 076015
[3] El-Guebaly L A (ARIES Team and FNSF Team) 2018 Nuclear assessment to support ARIES power plants and next-step facilities: emerging challenges and lessons learned *Fusion Sci. Technol.* **74** 340–69
[4] Reid J, Bailey G, Cracknell E, Gilbert M and Packer L 2021 Comparison of waste due to irradiated steels in the ESFR and DEMO *EPJ Web Conf.* **247** 18002

[5] Federici G, Biel W, Gilbert M R, Kemp R, Taylor N and Wenninger R 2017 European DEMO design strategy and consequences for materials *Nucl. Fusion* **57** 092002

[6] Bailey G W, Vilkhivskaya O V and Gilbert M R 2021 Waste expectations of fusion steels under current waste repository criteria *Nucl. Fusion* **61** 036010

[7] Gonzalez de Vicente S M *et al* 2022 Overview on the management of radioactive waste from fusion facilities: ITER, demonstration machines and power plants *Nucl. Fusion* **62** 085001

[8] Sublet J-C, Eastwood J W, Morgan J G, Gilbert M R, Fleming M and Arter W 2017 FISPACT-II: an advanced simulation system for activation, transmutation and material modelling *Nucl. Data Sheets* **139** 77–137

[9] Gilbert M R, Eade T, Bachmann C, Fischer U and Taylor N P 2018 Waste assessment of European DEMO fusion reactor designs *Fusion Eng. Des.* **136** 42–48

[10] Gilbert M R, Dudarev S L, Zheng S, Packer L W and Sublet J-C 2012 An integrated model for materials in a fusion power plant: transmutation, gas production and helium embrittlement under neutron irradiation *Nucl. Fusion* **52** 083019

[11] Hofmann F, Mason D R, Eliason J K, Maznev A A, Nelson K A and Dudarev S L 2015 Non-contact measurement of thermal diffusivity in ion-implanted nuclear materials *Sci. Rep.* **5** 16042

[12] Bhattacharya A, Zinkle S J, Henry J, Levine S M, Edmondson P D, Gilbert M R, Tanigawa H and Kessel C E 2022 Irradiation damage concurrent challenges with RAFM and ODS steels for fusion reactor first-wall/blanket: a review *J. Phys.: Energy* **4** 034003

[13] Gilbert M R *et al* 2021 Perspectives on multiscale modelling and experiments to accelerate materials development for fusion *J. Nucl. Mater.* **554** 153113

[14] Li S, Grossbeck M L, Zhang Z, Shen W and Chin B A 2011 The effect of helium on welding irradiated materials *Weld J.* **90** 19–26

[15] Fabritsiev S A and Pokrovsky A S 1998 The effect of helium accumulation and radiation damage on the weldability of 316-type steel *J. Nucl. Mater.* **258–263** 1991–6

[16] Maekawa F and Ikeda Y 2000 Decay heat experiment on thirty-two fusion reactor relevant materials irradiated by 14 MeV neutrons *Fusion Eng. Des.* **47** 377–88

[17] Maekawa F, Shibata K, Wada M, Ikeda Y and Takeuchi H 2002 Comprehensive activation experiment with 14 MeV neutrons covering most of naturally existing elements – 5 minutes irradiation experiment *J. Nucl. Sci. Technol.* **39** 990–3

[18] Sublet J-C 1998 Experimental validation of the decay power calculation code and nuclear database-FISPACT-97 and EAF-97, FENDL/A-2.0 *Technical Report* UKAEA-FUS-390, UKAEA available upon request from UKAEA

[19] Sublet J-C and Maekawa F 2009 Decay power: a comprehensive experimental validation *Technical Report* CEA-R-6213, CEA (available at: https://inis.iaea.org)

[20] Sublet J-C and Gilbert M R 2014 Decay heat validation, FISPACT-II & TENDL-2013,-2012 and EAF-2010 nuclear data libraries *Technical Report* CCFE-4(14)21, UKAEA (available at: http://fispact.ukaea.uk)

[21] Gilbert M R and Sublet J-C 2019 Experimental decay-heat simulation-benchmark for 14 MeV neutrons & complex inventory analysis with FISPACT-II *Nucl. Fusion* **59** 086045

[22] Gilbert M R, Vilkhivskaya O and Sublet J-C 2020 Fusion decay heat validation, FISPACT-II & TENDL-2019, ENDF/B-VIII.0, JEFF-3.3, EAF2010, and IRDFF-II nuclear data libraries *Technical Report* UKAEA-CCFE-RE(20)04, UKAEA (available at: http://fispact.ukaea.uk)

[23] Koning A J, Rochman D and Sublet J-C 2021 TENDL-2021 (available at: https://tendl.web.psi.ch/tendl_2021/tendl2021.html)

[24] Gilbert M R and Sublet J-C 2018 Fusion decay heat validation, FISPACT-II & TENDL-2017, EAF2010, ENDF/B-VIII.0, JEFF-3.3, and IRDFF-1.05 nuclear data libraries *Technical Report* CCFE-R(18)002, UKAEA (available at: http://fispact.ukaea.uk)

[25] Koning A J, Rochman D and Sublet J-C 2019 TENDL-2019 (available at: https://tendl.web.psi.ch/tendl_2019/tendl2019.html)

[26] The JEFF team 2017 JEFF-3.3: evaluated nuclear data library (available at: www.oecd-nea.org/dbdata/jeff/jeff33/index.html)

[27] Plompen A J M *et al* 2020 The joint evaluated fission and fusion nuclear data library, JEFF-3.3 *Eur. Phys. J.* A **56** 181

[28] Sublet J-C, Packer L W, Kopecky J, Forrest R A, Koning A J and Rochman D A 2010 The European activation file: EAF-2010 neutron-induced cross section library *Technical Report* CCFE-R(10)05 UKAEA (available at: https://scientific-publications.ukaea.uk)

[29] Brown D *et al* 2018 ENDF/B-VIII.0 nuclear data for science and technology (available at: www-nds.iaea.org/endfwww.nndc.bnl.gov/endf-b8.0/)

[30] Brown D A *et al* 2018 ENDF/B-VIII.0: the 8th major release of the nuclear reaction data library with CIELO-project cross sections, new standards and thermal scattering data *Nucl. Data Sheets* **148** 1–142

[31] Packer L W, Gilbert M R, Hughes S, Lilley S, Pampin R and Sublet J-C 2012 UK fusion technology experimental activities at the ASP 14 MeV neutron irradiation facility *Fusion Eng. Des.* **87** 662–6

[32] Packer L W, Hughes S, Gilbert M R, Lilley S and Pampin R 2013 Recent integral cross section validation measurements at the ASP facility *Fusion Eng. Des.* **88** 2617–20

[33] Lilley S, Packer L W, Pampin R and Gilbert M R 2013 Improved modelling of the neutron spectrum for the ASP accelerator *Fusion Eng. Des.* **88** 2627–30

[34] Gilbert M R, Packer L W and Lilley S 2014 Neutron irradiation experiments: automated processing and analysis of γ-spectra *Nucl. Data Sheets* **119** 401–3

[35] Packer L W, Gilbert M R and Lilley S 2014 Integral cross section measurements around 14 MeV for validation of activation libraries *Nucl. Data Sheets* **119** 173–5

[36] Stainer T, Gilbert M R, Packer L W, Lilley S, Gopakumar V and Wilson C 2021 14 MeV neutron irradiation experiments-gamma spectroscopy analysis and validation automation *EPJ Web Conf.* **247** 09010

[37] Gilbert M R, Packer L W and Stainer T 2020 Experimental validation of inventory simulations on molybdenum and its isotopes for fusion applications *Nucl. Fusion* **60** 106022

[38] Gilbert M R, Packer L W, Sublet J-C and Forrest R A 2014 Inventory simulations under neutron irradiation: visualization techniques as an aid to materials design *Nucl. Sci. Eng.* **177** 291–306

[39] Gilbert M R and Packer L W 2023 Developing a new validation benchmark for fusion inventory simulations *Nucl. Sci. Eng.* accepted

[40] Gilbert M R, Sublet J-C and Dudarev S L 2017 Spatial heterogeneity of tungsten transmutation in a fusion device *Nucl. Fusion* **57** 044002

[41] Hu X, Koyanagi T, Fukuda M, Kiran Kumar N A P, Snead L L, Wirth B D and Katoh Y 2016 Irradiation hardening of pure tungsten exposed to neutron irradiation *J. Nucl. Mater.* **480** 235–43

[42] Klimenkov M, Jäntsch U, Rieth M, Schneider H C, Armstrong D E J, Gibson J and Roberts S G 2016 Effect of neutron irradiation on the microstructure of tungsten *Nucl. Mater. Energy* **9** 480–3

[43] Abernethy R G *et al* 2019 Effects of neutron irradiation on the brittle to ductile transition in single crystal tungsten *J. Nucl. Mater.* **527** 151799

[44] Lloyd M J, Abernethy R G, Gilbert M R, Griffiths I, Bagot P A J, Nguyen-Manh D, Moody M P and Armstrong D E J 2019 Decoration of voids with rhenium and osmium transmutation products in neutron irradiated single crystal tungsten *Scr. Mater.* **173** 96–100

[45] Lloyd M J *et al* 2022 Interaction of transmutation products with precipitates, dislocations and grain boundaries in neutron irradiated W *Materialia* **22** 101370

[46] Edmondson P D, Gault B and Gilbert M R 2020 An atom probe tomography and inventory calculation examination of second phase precipitates in neutron irradiated single crystal tungsten *Nucl. Fusion* **60** 126013

[47] Bai H *et al* 2019 ^{56,54}Fe$(n, \alpha)^{53,51}$Cr cross sections in the MeV region *Phys. Rev.* C **99** 024619

[48] Otuka N *et al* EXFOR: experimental nuclear reaction data (https://doi.org/10.1016/j.nds.2014.07.065)

[49] Sterbenz S M *et al* 1994 The ^{56}Fe(n,xα) reaction from threshold to 30 MeV *Proc. Conf. on Nuclear Data for Science and Technology* (*Gatlinburg, TN, 9–13 May 1994*), vol 1 p 314

[50] Trkov A, Herman M and Brown D A 2018 ENDF-6 formats manual: data formats and procedures for the evaluated nuclear data files *Technical Report* BNL-203218-2018-INRE 1

[51] Koning A J and Rochman D 2012 Modern nuclear data evaluation with the TALYS code system *Nucl. Data Sheets* **113** 2841–934

[52] Koning A J, Rochman D, Sublet J C, Dzysiuk N, Fleming M and van der Marck S 2019 TENDL: complete nuclear data library for innovative nuclear science and technology *Nucl. Data Sheets* **155** 1–55

[53] Nobuta Y, Hatano Y, Matsuyama M, Abe S, Akamaru S, Yamauchi Y, Hino T, Suzuki S and Akiba M 2014 Tritium retention properties of tungsten, graphite and co-deposited carbon film *Fusion Eng. Des.* **89** 1516–9

[54] Windsor C G, Marshall J M, Morgan J G, Fair J, Smith G D W, Rajczyk-Wryk A and Tarragó J M 2018 Design of cemented tungsten carbide and boride-containing shields for a fusion power plant *Nucl. Fusion* **58** 076014

[55] Koyanagi T, Katoh Y, Nozawa T, Snead L L, Kondo S, Henager C H, Ferraris M, Hinoki T and Huang Q 2018 Recent progress in the development of SiC composites for nuclear fusion applications *J. Nucl. Mater.* **511** 544–55

[56] Forrest R A and Kopecky J 2002 The European activation file: EAF-2003 cross section library *Technical Report* UKAEA FUS 486

[57] Forrest R A 2002 The European activation system: EASY-2003 overview *Technical Report* UKAEA FUS 484 (available at: https://scientific-publications.ukaea.uk)

[58] Forrest R A 2002 FISPACT-2003: user manual *Technical Report* UKAEA FUS 485

[59] Gilbert M R and Sublet J-C 2016 Handbook of activation, transmutation, and radiation damage properties of the elements simulated using FISPACT-II & TENDL-2015; Magnetic fusion plants *Technical Report* CCFE-R(16)36, UKAEA (available at: http://fispact.ukaea.uk)

[60] Koning A J *et al* 2016 TENDL-2015 (available at: https://tendl.web.psi.ch/tendl_2015/tendl2015.html)

[61] Vilkhivskaya O and Gilbert M 2021 Nuclear data V&V analysis for fusion applications: integral benchmarks and decay data *EPJ Web Conf.* **247** 10015

[62] Vilkhivskaya O 2020 Decay-2020: an updated general purpose decay data library (available at: fispact.ukaea.uk)

[63] Rising M E *et al* 2023 MCNP® code version 6.3.0 release notes *Technical Report* LA-UR-22-33103, Rev. 1 (Los Alamos, NM: Los Alamos National Laboratory)

[64] Romano P K, Horelik N E, Herman B R, Nelson A G, Forget B and Smith K 2015 OpenMC: a state-of-the-art Monte Carlo code for research and development *Ann. Nucl. Energy* **82** 90–97

[65] Kodeli I A and Sartori E 2021 SINBAD–radiation shielding benchmark experiments *Ann. Nucl. Energy* **159** 108254

[66] Batistoni P *et al* 2010 Neutronics experiments on HCPB and HCLL TBM mock-ups in preparation of nuclear measurements in ITER *Fusion Eng. Des.* **85** 1675–80

[67] Flammini D, Angelone M, Caiffi B, Colangeli A, Fonnesu N, Mariano G, Moro F and Villari R 2020 Pre-analysis of the WCLL breeding blanket mock-up neutronics experiment at the frascati neutron generator *Fusion Eng. Des.* **156** 111600